

A&A manuscript no.  
(will be inserted by hand later)

Your thesaurus codes are:  
02.01.1; 02.18.5; 08.19.5 Cas A; 13.07.3; 13.18.3

ASTRONOMY  
AND  
ASTROPHYSICS

# On the gamma-ray fluxes expected from Cassiopeia A

A. M. Atoyan<sup>1,2</sup>, F. A. Aharonian<sup>1</sup>, R. J. Tuffs<sup>1</sup>, and H. J. Völk<sup>1</sup>

<sup>1</sup> Max Planck Institut für Kernphysik, Saupfercheckweg 1, D-69117 Heidelberg, Germany

<sup>2</sup> Yerevan Physics Institute, 375036 Yerevan, Armenia

Received 6 July ; accepted 12 Dec 1999

**Abstract.** Based on the results of our previous study of the broad band synchrotron emission of Cas A in the framework of a spatially inhomogeneous model, we calculate the fluxes of  $\gamma$ -radiation that can be expected from this supernova remnant in different energy bands. We show that at energies below 10 GeV  $\gamma$ -ray fluxes detectable by forthcoming space-borne detectors should be inevitably produced due to bremsstrahlung of radio emitting electrons. We predict that the power-law index of the photon flux in the GeV region should be hard, close to the index  $\beta_{\text{acc}} \sim 2.2$  expected for the acceleration spectrum of electrons in compact bright radio structures. Photon fluxes accessible to future ground-based  $\gamma$ -ray detectors could also be expected at very high energies. The fluxes to be expected due to bremsstrahlung and inverse Compton radiation of relativistic electrons at TeV energies should be very steep, and strongly dependent on the characteristic magnetic fields in Cas A. We could expect also significant fluxes of  $\pi^0$ -decay  $\gamma$ -rays produced by relativistic protons which presumably are also accelerated in Cas A. These fluxes may extend with a hard spectrum beyond TeV energies as far as the protons could be accelerated to energies  $\geq 100$  TeV. The hardness of the  $\gamma$ -ray spectrum at TeV energies could in principle allow one to distinguish between electronic and hadronic origins of those  $\gamma$ -rays. We discuss also other implications, such as relativistic particle content, or physical parameters in the source, that could be derived from future  $\gamma$ -ray flux measurements in different energy bands.

**Key words:** acceleration of particles – radiation mechanisms: non-thermal – supernovae: individual: Cas A – gamma-rays: theory – radio continuum: ISM

## 1. Introduction

The shell type supernova remnant (SNR) Cassiopeia A is a prominent source of nonthermal radiation in the Galaxy. It is the brightest and one of the best studied radio sources

(e.g. Bell 1975; Tuffs 1986; Braun et al. 1987; Anderson et al. 1991; Kassim et al. 1995; etc.), with synchrotron radiation fluxes observed also at sub-millimeter wavelengths (Mezger et al. 1986), and probably even further in the near infrared (Tuffs et al. 1997) and at hard X-ray energies (Allen et al. 1997; Favata et al. 1997). The powerful radio emission of Cas A implies a total energy in relativistic electrons of order  $10^{48}$  erg or higher (e.g. Chevalier et al. 1978; Anderson et al. 1991). A synchrotron origin of hard X-rays implies that relativistic electrons are accelerated up to energies of a few tens of TeV (Allen et al. 1997; Favata et al. 1997). Thus, one should also expect the production of non-thermal  $\gamma$ -rays in Cas A, due to the bremsstrahlung and inverse Compton (IC) mechanisms, extending possibly beyond TeV energies. However, in the MeV  $\gamma$ -ray domain only the  $^{44}\text{Ti}$  line emission at an energy of 1.157 MeV has been detected by COMPTEL (Iyudin et al. 1994). High energy  $\gamma$ -ray observations of Cas A by EGRET resulted in the flux upper limit  $I(> 100 \text{ MeV}) \leq 1.2 \times 10^{-7} \text{ ph/cm}^2\text{s}$  (Esposito et al. 1996). At TeV energies flux upper limits have been given by the Whipple (Lessard et al. 1999) and CAT (Goret et al. 1999) collaborations. A tentative detection of a weak signal at a significance level of  $\simeq 5\sigma$  has been recently reported by the HEGRA collaboration (Pühlhofer et al. 1999).

Gamma-ray fluxes expected from Cas A have been earlier calculated by Cowsik & Sarkar (1980) who have derived a lower limit to the mean magnetic field in the shell of Cas A,  $B_0 \geq 8 \times 10^{-5} \text{ G}$ , comparing the bremsstrahlung flux of radio emitting electrons with the upper flux limit  $I(> 100 \text{ MeV}) \leq 1.1 \times 10^{-6} \text{ ph/cm}^2\text{s}$  of SAS-2 (Fichtel et al. 1975) and COS B detectors. Calculations have been done in a commonly used ‘single-zone’ model approximation, which assumes a spatially homogeneous source containing magnetic field, relativistic electrons and gas. In the same single-zone approximation, broad-band fluxes of  $\gamma$ -rays expected from Cas A have been recently calculated by Ellison et al. (1999) and Goret et al. (1999).

In our previous work (Atoyan et al. 1999, hereafter Paper 1) we have carried out detailed modelling of the synchrotron radiation of Cas A from the radio to the X-ray bands in order to understand the relativistic electron

content in the source. The principal feature of our study in Paper 1 was that we have proposed a *spatially inhomogeneous* model, consisting of two zones, that distinguishes between compact, bright steep-spectrum radio knots and the bright fragmented radio ring on the one hand, and the remainder of the shell - the diffuse ‘plateau’ - on the other hand. In this paper, using the model parameters derived from the interpretation of synchrotron fluxes observed, we calculate the fluxes of  $\gamma$ -rays predicted in the framework of the spatially inhomogeneous study of this SNR, and discuss implications which can be derived from future  $\gamma$ -ray observations of this SNR in different energy bands. In section 2, after a brief overview of the basic features of the model, we study the fluxes to be expected for  $\gamma$ -ray energies up to  $E \sim 10 - 100$  GeV. This emission is contributed mostly by bremsstrahlung of those electrons which are responsible for the synchrotron emission in the radio-to-infrared bands. In section 3 we discuss the fluxes expected in the very high energy region,  $E \geq 100$  GeV, where both bremsstrahlung and inverse Compton radiation of relativistic electrons are important. In addition, a significant contribution to the total fluxes could be due to  $\pi^0$ -decay  $\gamma$ -rays. These should originate from relativistic protons which presumably are also accelerated in Cas A. A summary and the conclusions are contained in section 4.

## 2. High energy bremsstrahlung of radio electrons

### 2.1. Overview of the model

In Paper 1 we have shown that the basic features of the observed radio emission, in particular,

- (a) spectral turnover of the energy fluxes  $J_\nu \sim \nu^{-\alpha}$  at frequencies below 20 MHz,
- (b) mean spectral index  $\alpha \approx 0.77$  of the total flux at higher frequencies up to  $\nu \leq 30$  GHz (e.g. Baars et al. 1977) which then flattens to  $\alpha \approx 0.65$  in the submillimeter domain (Mezger et al. 1986),
- (c) the spread of spectral indices of the radio knots from  $\alpha \sim 0.6$  to  $\alpha \sim 0.9$  (Anderson and Rudnick, 1996),

and other characteristics can be explained in the framework of a model that takes into account the effects of energy dependent propagation of relativistic electrons in a spatially nonuniform remnant. We have considered the simplest inhomogeneous model, consisting of two zones with essentially different spatial densities of relativistic electrons. The model allows a rather clear qualitative and quantitative distinction between compact bright radio structures in Cas A like the fragmented radio ring and the radio knots on the one hand, and the remainder of the radio emitting shell - the diffuse radio ‘plateau’ region enclosed between the radio ring at  $R_{\text{ring}} \approx 1.7$  pc and the blast wave at  $R_0 \approx 2.5$  pc (for a distance  $d = 3.4$  kpc to Cas A, cf. Reed et al. 1995) - on the other. The model predicts that the spatial density of relativistic electrons in

the compact radio structures, which all together constitute what we termed zone 1, is much higher than in the surrounding plateau region, termed zone 2. Thus, zone 1 with a total volume  $V_1$  much smaller than the volume  $V_0$  of the shell is actually merged into zone 2 with a volume  $V_2 = V_0 - V_1 \approx V_0$ .

In Paper 1 we have derived, by spatial integration of the diffusion equation for relativistic electrons, the set of Leaky-box type equations for the overall energy distribution functions of the electrons  $N_1(E, t)$  and  $N_2(E, t)$  in zones 1 and 2, respectively. We do not consider the acceleration process itself, but assume that the accelerated electrons are injected into zone 1 with some rate  $Q(E, t)$ , and study the effects of the energy-dependent diffusive propagation of the particles on their spectra  $N_{1,2}(E, t)$ . Such a phenomenological approach is justified if particle acceleration occurs in a volume significantly smaller than the volume where the bulk of the emission of zone 1 is produced. The equation for zone 1 then reads:

$$\frac{\partial N_1}{\partial t} = \frac{\partial(P_1 N_1)}{\partial E} - \frac{N_1}{\tau_{\text{esc}}} + \frac{V_1 N_2}{V_2 \tau_{\text{dif}}} + Q, \quad (1)$$

where  $P_1$  represents the energy loss rate of the electrons in zone 1. The second term on the right hand side of Eq.(1) describes the escape of the electrons into the plateau region on timescales

$$\tau_{\text{esc}}(E) = \left[ \frac{1}{\tau_{\text{dif}}(E)} + \frac{1}{\tau_c} \right]^{-1}. \quad (2)$$

The term  $\tau_c \sim 2R_1/u_1$ , where  $R_1 \sim (0.03 - 0.1)$  pc is a typical radius of the compact radio components and  $u_1$  is the fluid speed in zone 1, corresponds to the convective escape time which does not depend on the electron energy. The principal energy dependent term in Eq.(2) is the diffusive escape time:

$$\tau_{\text{dif}}(E) = \tau_* (E/E_*)^{-\delta} + \tau_{\text{min}}, \quad (3)$$

where normalization to a typical energy  $E_* = 1$  GeV of radio emitting electrons is used, and  $\tau_{\text{min}} = 2R_1/c$  takes into account that the escape time cannot be shorter than the light travel time.

The third term on the right hand side of Eq.(1) takes into account that the diffusive propagation and escape of particles is effectively possible only in the directions opposite to the gradients of their spatial density, i.e. from zone 1 with a high concentration of radio electrons into zone 2. In a standard power-law approximation for the above source function

$$Q(E) = Q_0 E^{-\beta_{\text{acc}}} \exp(-E/E_c), \quad (4)$$

the spectrum of the accelerated electrons can be hard,  $\beta_{\text{acc}} \simeq 2.2$ . However the energy distribution  $N_1(E)$  of radio electrons in zone 1 becomes steeper than  $Q(E)$  on the timescale  $\tau_{\text{esc}}(E)$  of electron escape from zone 1 into zone 2. It is important that, as shown in Paper 1, the

degree of steepening at energy  $E$  essentially depends on the ratio (or ‘the gradient’) of the energy densities of the electrons  $N_1(E)/V_1$  to  $N_2(E)/V_2$  in these two zones. The maximum steepening, corresponding to the spectrum  $N_1(E) \simeq Q(E) \times \tau_{\text{esc}}(E) \propto E^{-\beta_{\text{max}}}$  with  $\beta_{\text{max}} = \beta_{\text{acc}} + \delta$ , is reached only if this gradient is very high, and there is *no steepening at all* if the energy densities become equal. Therefore, although the two-zone model is also rather simplified, as compared with the reality, because it assumes the same electron density for all components in zone 1, it allows a qualitative explanation for the variations of the power-law indices of individual radio knots from  $\alpha_{\text{min}} \simeq 0.6$  to  $\alpha_{\text{max}} \simeq 0.9 - 0.95$  (Anderson & Rudnick 1996; see also Wright et al. 1999) assuming an efficient electron acceleration with the same hard power-law spectrum  $\beta_{\text{acc}} = 1 + 2\alpha_{\text{min}} \simeq 2.2$  and a diffusive escape time with a parameter  $\delta \simeq 0.6 - 0.7$ . These variations do not then necessarily imply that particle acceleration significantly varies across the remnant (Wright et al. 1999), but can be explained rather by differences in the local gradients, with respect to the surrounding plateau, of the concentration of radio electrons for different members of zone 1.

In Paper 1 we have shown that a high contrast of electron densities needed for interpretation of the radio observations can be reached if the zone 1 components correspond to the sites of efficient electron acceleration. In principle, the interpretation of the radio data of Cas A does not suggest an efficient acceleration of the electrons in zone 2. We note however that such an acceleration, with similarly hard power-law index  $\beta_{\text{acc}}$  as in zone 1, is not excluded, provided that the amount of radio electrons accelerated directly in the plateau region does not significantly exceed the number of electrons leaking into zone 2 from zone 1. Otherwise the gradients in the spatial densities of electrons would be reduced resulting then in a strong suppression of spectral modifications of  $N_1(E, t)$  in the zone 1 regions.

The equation for the electron distribution  $N_2(E, t)$  in zone 2 is similar to Eq.(1), where the source function  $Q$  is substituted by  $Q_2 = N_1/\tau_{\text{esc}}$  (taking into account that effectively the escape of relativistic electrons from zone 1 corresponds to their injection into zone 2, and neglecting possible acceleration in zone 2), and the sign of the term  $V_1 N_2/V_2 \tau_{\text{dif}}$  which describes the diffusive escape of electrons from zone 2 into zone 1 is changed. Note that a two-zone model does not assume any other escape of electrons from zone 2, e.g. into regions outside of the shell, because otherwise such an escape would correspond to a three-zone model (see Sect. 3 below).

Numerical calculations are done by the method of iterations using general analytical solutions to the Leaky-box type equations (e.g. see Atoyan & Aharonian 1999). For

example, the solution for Eq.(1) can be presented as

$$N_1(E, t) = \frac{1}{P_1(E)} \int_0^t P_1(\zeta_t) Q_{\text{eff}}(\zeta_t, t_1) \times \exp\left(-\int_{t_1}^t \frac{dx}{\tau_{\text{esc}}(\zeta_x)}\right) dt_1, \quad (5)$$

where  $Q_{\text{eff}}(E, t) = Q + N_2/\tau_{\text{esc}}$ . The variable  $\zeta_t$  corresponds to the energy of an electron at instant  $t_1 \leq t$  which has the energy  $E$  at the instant  $t$ , and is determined from the equation

$$t - t_1 = \int_{E_e}^{\zeta_t} \frac{dE}{P_1(E)}. \quad (6)$$

At the first step of the iteration procedure a function  $N_1^{(1)}(E)$  corresponding to the first approximation of  $N_1$  is calculated for an injection function  $Q$  in the form of Eq.(4), i.e. neglecting the term  $N_2/\tau_{\text{esc}}$  in  $Q_{\text{eff}}(E)$ , or else - neglecting in Eq.(1) the term describing the diffusive ‘return’ flux of the electrons from zone 2 into zone 1. Then the energy distribution of the electrons  $N_2^{(1)}(E)$  in zone 2 in the first approximation, corresponding to an effective injection function of the electrons in this zone  $N_1^{(1)}(E)/\tau_{\text{esc}}(E)$ , is found. After that  $N_2^{(1)}(E)$  is used for calculations of  $N_1^{(2)}(E)$  in zone 1 in the second approximation, which now takes into account the ‘return’ flux of the electrons from zone 2. Calculations show that such a simple iteration procedure is quickly converging, so typically several iterations are sufficient to reach a good accuracy in the final electron distributions  $N_1$  and  $N_2$ .

The characteristics of the broad band synchrotron radiation of Cas A can be best explained for the mean magnetic fields  $B_1 \simeq (1 - 2)$  mG and  $B_2 \simeq (0.3 - 0.5)$  mG in zones 1 and 2, respectively. The total energy content in relativistic electrons in each of these zones is of order  $10^{48}$  erg, depending on the magnetic fields  $B_1$  and  $B_2$ . The X-ray fluxes observed above 10 keV can be explained by synchrotron radiation of electrons in zone 1 with an exponential cutoff energy  $E_c \simeq (15 - 30)$  TeV in Eq.(4).

A possible fit to the broad band synchrotron fluxes of Cas A is shown in Fig. 1. Magnetic fields  $B_1 = 1.2$  mG and  $B_2 = 0.3$  mG in the compact bright radio structures and in the diffuse plateau region, respectively, are assumed. The total magnetic field energy in the shell is then  $W_{B2} = 3.8 \times 10^{48}$  erg, and in the compact zone 1 regions it is  $W_{B1} = 2 \times 10^{47}$  erg. The total energy of electrons in zones 1 and 2 is  $W_{e1} = 1.6 \times 10^{48}$  erg and  $W_{e2} = 1.8 \times 10^{48}$  erg, respectively.

The energy distributions of the electrons  $N_1(E)$  and  $N_2(E)$  formed in zones 1 and 2, as well as the overall distribution  $N_{\text{tot}}(E) = N_1(E) + N_2(E)$ , are shown in Fig. 2. As expected,  $N_{\text{tot}}(E)$  shows a pure power-law behavior with  $\beta = \beta_{\text{acc}}$  until the so-called ‘radiative break’ energy  $\simeq 500$  GeV. At this energy the synchrotron cooling time of the electrons in zone 2

$$t_s \approx 300 (E/1 \text{ TeV})^{-1} (B_2/0.2 \text{ mG})^{-2} \text{ yr} \quad (7)$$

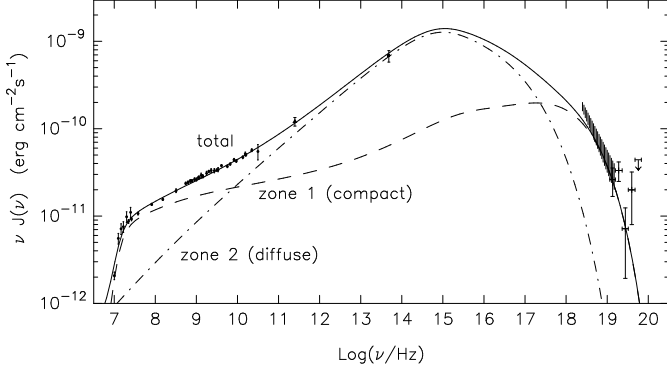


**Fig. 1.** Synchrotron fluxes calculated in the framework of two-zone model for Cas A. An acceleration spectrum of the electrons in the zone 1, which is modelled as being composed of  $K = 150$  compact structures with a mean radius  $R = 0.06$  pc is given by Eq.(4) with the power law index  $\beta_{\text{acc}} = 2.2$  and exponential cutoff energy  $E_c = 18$  TeV; escape of the electrons into the surrounding extended zone 2 is described by Eqs. (2) and (3), with parameters  $\tau_* = 28$  yr and  $\delta = 0.7$ . The magnetic fields in zones 1 and 2 are  $B_1 = 1.2$  mG and  $B_2 = 0.3$  mG, respectively. Dashed and dot-dashed curves show contributions of zone 1 and zone 2 into the overall synchrotron radiation flux (solid). The fluxes of Cas A measured from radio to soft  $\gamma$ -ray bands (see Paper 1 for relevant references) are also shown.

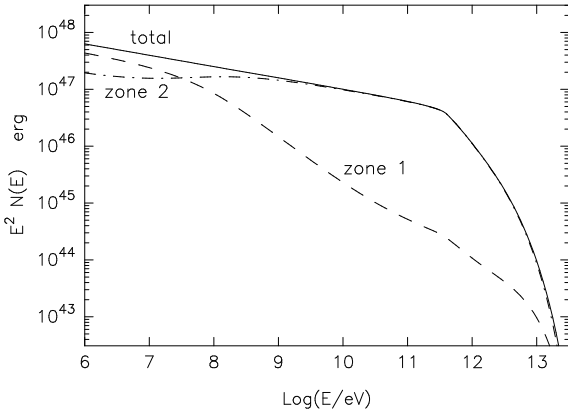


**Fig. 2.** The energy distributions of relativistic electrons  $N_1(E)$  and  $N_2(E)$  in zone 1 (dashed line) and zone 2 (dot-dashed line) which correspond to Fig.1. The solid line shows the total energy distribution of electrons in the source.

becomes equal to the age of the source, and at higher energies the radiative losses steepen the spectrum of zone 2 electrons to the power-law index  $\beta = \beta_{\text{acc}} + 1$ . Meanwhile, at  $E \geq 100$  MeV the energy distribution of radio electrons in zone 1 is steepened to  $\beta_1 \simeq \beta_{\text{acc}} + \delta$  because of diffusive escape of the electrons from that zone where their spatial density  $n_1(E) = N_1(E)/V_1$  is much higher than  $n_2(E) = N_2(E)/V_2$  in the surrounding plateau region.

## 2.2. Gamma-ray emission

The photon flux  $I(E) = J(E)/E$  of the bremsstrahlung  $\gamma$ -rays at energies  $E \gg m_e c^2$  practically repeats the power-law spectral shape of the parent electrons. Therefore, one might expect that  $I(E)$  would have the same power-law index  $\alpha_{\text{dif}} = \alpha + 1 \approx \beta_{\text{acc}}$  as  $N_{\text{tot}}(E)$ . However because of the different spectral shapes of the radio electrons in zones 1 and 2 where, most probably, the gas densities are also different, the total bremsstrahlung spectrum of Cas A can somewhat deviate from the power-law behavior of the injection spectrum.

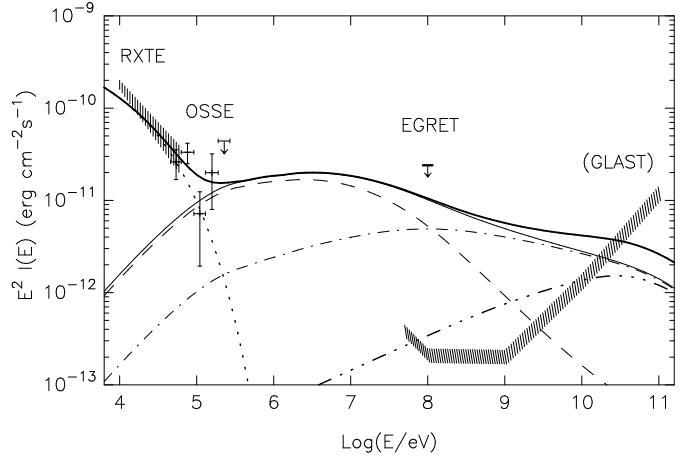


**Fig. 3.** The fluxes of synchrotron (dotted line), bremsstrahlung (thin solid line) and inverse Compton (3-dot-dashed line) radiations calculated in the framework of two-zone model for the same model parameters as in Fig. 1. The dashed and dot-dashed curves correspond to the bremsstrahlung fluxes produced in zone 1 and zone 2, respectively. The heavy solid curve is the overall flux. The hatched region shows the expected flux sensitivity of GLAST (Bloom 1996). The X-ray/soft  $\gamma$ -ray fluxes measured by RXTE (Allen et al. 1997) and OSSE (The et al. 1996) detectors, as well as flux upper limit of EGRET (Esposito et al. 1996) are also shown.

In Fig.3 the thin solid line corresponds to the total flux of the bremsstrahlung photons produced by the electrons shown in Fig.2, and the dashed and dot-dashed lines represent the fluxes from zone 1 and zone 2, respectively. For the calculations we adopt a mean gas density  $n_{\text{H},2} = 15 \text{ cm}^{-3}$  in terms of ‘H-atoms’ (i.e. the nucleons) in zone 2. This corresponds to a total mass of about  $15 M_{\odot}$  (e.g. Fabian et al. 1980; Jansen et al. 1988; Vink et al. 1998), in the volume  $V \approx 1.2 \times 10^{57} \text{ cm}^3$  of the shell between  $R_{\text{ring}}$  and  $R_0$ . The mean value of the parameter  $C_Z = Z(Z+1)/A$  in the oxygen-rich ( $Z = 8$ ,  $A = 16$ ) gas in the shell (zone 2) of Cas A derived by Cowsik & Sarkar (1980) is  $\overline{C_Z} = 4.3$ . For zone 1 we assume the same atomic  $\overline{C_{Z,1}} = 4.3$ , and the gas density  $n_{\text{H},1} = 4n_{\text{H},2}$ . We note however that these parameters in the compact radio

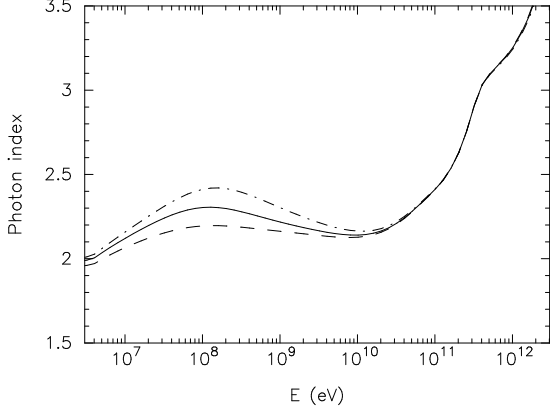


**Fig. 4.** The spectral indices of the photon flux  $I(E)$  of the broad-band  $\gamma$ -radiation expected from Cas A in the case of 3 different ratios of the gas parameter  $n_{\text{H}} \overline{C_Z}$  in the compact zone 1 structures and extended zone 2 (the shell). The solid curve corresponds to the ratio  $n_{\text{H},1} \overline{C_{Z,1}}/n_{\text{H},2} \overline{C_{Z,2}} = 4$ , as assumed for the calculations in Fig. 3, whereas the dashed and dot-dashed curves show the spectral photon indices which result if this ratio is equal, respectively, to 2 and 8.

structures are not known. In particular, the radio knots show practically no optical line emission which would allow conclusions about the density and mass composition of the gas there. Therefore, for different values of the gas parameters in zone 1, the relative contribution of zones 1 and 2 to the total bremsstrahlung flux would change. As shown in Fig.4, this results in some uncertainty of the model predictions for the steepness of the total  $\gamma$ -ray fluxes at energies  $E \sim 100$  MeV. At both smaller ( $\leq 10$  MeV) and higher ( $\geq 1$  GeV) energies, where the bremsstrahlung flux is contributed mainly either by the first or by the second zone, the spectral indices are much less affected by the uncertainty in the gas parameters in zone 1.

Because of the steep decline of the energy distribution of radio electrons in the compact zone 1 structures, the intensity of the  $\gamma$ -ray flux at  $E \sim 1$  GeV is dominated by the flat-spectrum bremsstrahlung of zone 2 (see Fig.3). It is also important that the contribution of the IC radiation, discussed in detail in the next section, at this energy is not yet significant. Therefore, measurements of the differential flux  $I(E)$  of high energy  $\gamma$ -rays from Cas A by the future GLAST detector should allow a rather accurate determinations of a number of important parameters in Cas A. In particular, the spectral index of  $I(E)$  at GeV energies could give rather accurate information about the spectrum of electrons in zone 2,  $\alpha_{\text{dif}} \approx \beta_2$  (see Figs. 3 and 4). At these energies the energy distribution of electrons in zone 2 has a power law distribution  $N_2(E) \propto E^{-\beta_2}$  with the spectral index of accelerated particles,  $\beta_2 = \beta_{\text{acc}}$  (see Fig.2).

Bremsstrahlung  $\gamma$ -rays with energies  $E_\gamma \simeq 1$  GeV are produced by electrons with characteristic energies  $E_e \sim$

$2 E_\gamma$ . The mean frequency of the synchrotron photons emitted by the same electrons is  $\nu \simeq 10^3 B_{\text{mG}} (E_e/m_e c^2)^2$  where  $B_{\text{mG}} = B/1$  mG (e.g. Ginzburg 1979). In terms of the  $\gamma$ -ray energy this relation is reduced to

$$\nu \simeq 4 B_{\text{mG}} (E_\gamma/1 \text{ GeV})^2 \text{ GHz}. \quad (8)$$

For the expected mean magnetic field in the shell of Cas A of about (0.3–0.5) mG (Paper 1), electrons responsible for bremsstrahlung of (1–2) GeV  $\gamma$ -rays are also producing synchrotron photons with  $\nu \sim$  few GHz. Thus, a comparison of the radiation intensities in these two regions will give almost model independent information about the mean magnetic field  $B_2$  in the shell.

Indeed, for the power-law distribution of electrons  $N(E) \propto E^{-\beta}$ , the intensity of synchrotron radiation can be written in the form (see Paper 1):

$$J_\nu \simeq 1.5 \times 10^3 \left( \frac{N_*}{10^{50}} \right) \left( \frac{B}{1 \text{ mG}} \right)^{\frac{1+\beta}{2}} \times \left( \frac{\nu}{10 \text{ GHz}} \right)^{\frac{1-\beta}{2}} \left( \frac{d}{3.4 \text{ kpc}} \right)^{-2} \text{ Jy}, \quad (9)$$

where  $N_* \equiv E_* N(E_*)$ , with  $E_* = 1$  GeV, is the characteristic total number of 1 GeV electrons. The bremsstrahlung intensity  $I(E)$  (see e.g. Blumenthal and Gould 1970) can be presented in the form of an energy flux  $f(E) = E^2 I(E)$  as

$$f(E) \simeq 7.5 \times 10^{-15} n_{\text{H}} \overline{C_Z} 2^{2-\beta} \left( \frac{N_*}{10^{50}} \right) \left( \frac{E}{1 \text{ GeV}} \right)^{2-\beta} \times \left[ \ln \left( \frac{E}{1 \text{ GeV}} \right) + 8.4 \right] \left( \frac{d}{3.4 \text{ kpc}} \right)^{-2} \frac{\text{erg}}{\text{cm}^2 \text{ s}}, \quad (10)$$

where  $\overline{C_Z} = \overline{Z(Z+1)/A}$ , as previously. Then, because the total intensity of  $\gamma$ -rays at (1–2) GeV is dominated by the bremsstrahlung of radio electrons in the shell (zone 2) responsible also for the diffuse ‘radio plateau’ emission at  $\nu \sim 5$  GHz with the known flux  $J_2(\nu)$ <sup>1</sup>, and because the value of  $n_{\text{H},2} \overline{C_{Z,2}}$  in the shell is known with sufficient accuracy, comparison of equations (9) and (10) will result in a rather accurate estimate of the magnetic field  $B_2$ . For example, in the case of  $\alpha_{\text{dif}} \simeq \beta_{\text{acc}} \sim 2.2$  as expected, the mean magnetic field in the shell would be

$$B_2 \approx 0.16 \left[ \frac{J_2(5 \text{ GHz})}{350 \text{ Jy}} \right]^{0.63} \left[ \frac{f(1 \text{ GeV})}{10^{-11} \text{ erg/cm}^2 \text{ s}} \right]^{-0.63} \text{ mG} \quad (11)$$

This knowledge of  $B_2$  could then help to estimate the mean magnetic field also in compact bright radio structures as  $B_1 \sim 4 B_2$  which is needed for interpretation of the radio data (see Paper 1).

<sup>1</sup> The measurements of Tuffs (1986) taken in 1978 have shown that  $\approx 50\%$  of the total flux  $J(\nu) \approx 800$  Jy of Cas A was due to plateau emission. Taken into account the secular decline of the fluxes, the intensity of diffuse radio emission presently can be estimated as  $J_2(5 \text{ GHz}) \sim 350$  Jy.

At energies  $\leq 100$  MeV the overall flux of  $\gamma$ -rays is dominated by the bremsstrahlung of relativistic electrons in the compact zone 1 region. As follows from Eq.(8), the radio counterpart of the  $E \sim 100$  MeV  $\gamma$ -rays is the region of frequencies  $\nu \sim 40$  MHz, where the synchrotron radiation is dominated by zone 1 emission (see Fig.1), and the fluxes are not yet affected by synchrotron self-absorption. Although the expected flux sensitivity of the GLAST detector drops significantly below 100 MeV, in principle it may be able to detect  $\gamma$ -ray fluxes down to energies  $\sim 10$  MeV (Bloom 1996). Detailed modelling of the flux  $I(E)$  would help to extract the intensity of 100 MeV bremsstrahlung  $\gamma$ -rays produced in zone 1, i.e. in the bright radio ring and radio knots. Then, for known  $I_1(E \sim 100$  MeV),  $J_1(\nu = 40$  MHz), and  $\beta = \beta_1 \sim (2.7 - 2.8)$  in zone 1 (as predicted in Paper 1), the equations (9) and (10) can be used to derive the unknown product ( $n_H \times \overline{C_Z}$ ) there. Note that in principle the gas parameters can be different in the radio ring and radio knots. A possibility of separation of the contributions of these two different sub-components of zone 1 to the overall flux  $I_1(E)$  could enable determination of the product  $n_H \overline{C_Z}$  in each of them.

Important additional information about the gas parameters in compact components could be derived from future observations of Cas A with high angular and energy resolution by the X-ray telescopes Chandra, XMM and Astro-E in the keV region. Even for the case of non-detection of the line features from radio knots, the intensity of their *thermal* X-ray emission will help to disentangle the density  $n_H$  from the mean abundance  $\overline{C_Z}$ . Because the intensity of thermal emission  $Q_T \propto \overline{Z^2} n_Z n_e \simeq \overline{C_Z} n_H n_e$ , and because for the ionized gas the thermal electron density  $n_e = Z n_Z \simeq n_H/2$  (except for a hydrogen-dominated medium where  $n_e \simeq n_H$ ), the fluxes of thermal X-rays will in principle allow determination of the parameter  $\overline{C_Z} n_H^2$  in the zone 1 structures. When combined with the knowledge of a different product of parameters  $\overline{C_Z}$  and  $n_H$  found from the comparison of  $\gamma$ -ray with synchrotron measurements, each of these two parameters could be found.

### 3. Gamma-ray emission at very high energies

#### 3.1. Emission of relativistic electrons

If the fluxes of hard X-rays observed at  $E \geq 10$  keV have a synchrotron origin (Allen et al. 1997, Favata et al. 1997; – but see also Laming 1998), relativistic electrons in Cas A should be accelerated to energies up to tens of TeV. These electrons should then produce very high energy (VHE,  $E \geq 100$  GeV)  $\gamma$ -rays. Along with bremsstrahlung, at these energies the principal mechanism for  $\gamma$ -ray production is the inverse Compton (IC) scattering of the electrons in the ambient soft photon field. In principle, the photon field is contributed by the synchrotron photons, the thermal dust emission with  $T = 97$  K (Mezger et al. 1986) in the far infrared (FIR), the optical/IR line photons, and the 2.7 K cosmic microwave background radiation.

As shown in Fig.5, the most important target photon field for production of IC  $\gamma$ -rays in Cas A is the FIR radiation which is responsible for  $\geq 80\%$  of the IC flux in the VHE region. Note that only due to the high density of the FIR radiation in Cas A (which has not been taken into account in recent calculations by Ellison et al. 1999), the flux of IC  $\gamma$ -rays becomes comparable at TeV energies with the bremsstrahlung flux. Because the photon fields should have practically the same density in both compact and diffuse zones, irrespective of where they are produced, and since the VHE electrons reside mostly in zone 2 (see Fig. 2), IC radiation is contributed mostly by this zone. For an assumed mean magnetic field in the shell  $B_2 = 0.3$  mG (Fig.5), the energy density of the magnetic field is  $w_B = 2.5 \times 10^3$  eV/cm<sup>3</sup>, whereas the density of the FIR radiation calculated for the luminosity  $L_{\text{FIR}} \approx 3.6 \times 10^{37}$  erg/s (Mezger et al 1986) is only  $w_{\text{rad}} \simeq 2$  eV/cm<sup>3</sup>. Because the ratio of synchrotron to IC (in the Thomson limit) emissivities

$$q_{\text{sy}}/q_{\text{IC}} = w_B/w_{\text{rad}} \propto B^2, \quad (12)$$

the IC fluxes of VHE  $\gamma$ -rays are  $\simeq 10^3$  times lower than the fluxes of synchrotron radiation produced by the same parent electrons in the UV/X-ray region.

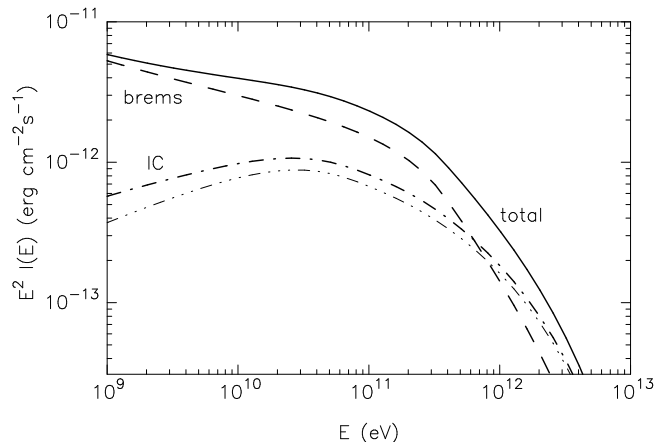


**Fig. 5.** The fluxes of bremsstrahlung (dashed) and IC (dot-dashed)  $\gamma$ -rays calculated in the framework of two-zone model for Cas A for the same model parameters as in Fig.1. The solid curve corresponds to the total flux. The thin 3-dot-dashed curve shows the fraction of IC  $\gamma$ -rays produced due to upscattering of the thermal dust photons; other target photons for IC scattering of electrons are the synchrotron radiation, 2.7 K microwave background radiation, and optical line emission of Cas A.

The fluxes of IC  $\gamma$ -rays to be expected from Cas A depend very sensitively on the mean magnetic field  $B_2$  in the shell. As follows from Eq.(9), an increase of  $B_2$  by a factor  $a$  reduces the total number of electrons needed for explanation of the radio fluxes observed by a factor  $a^{(1+\beta_2)/2}$ . This results in a strong decrease of the bremsstrahlung

flux by the same factor, i.e.  $f_{\text{br}} \propto 1/a^{(1+\beta_2)/2}$ . The same dependence on the magnetic field also holds for the intensity of IC emission which is produced by the electrons below the radiative break energy (the ‘knee’ around 500 GeV in Fig.2) for which the synchrotron cooling time is larger than the age  $t_0$  of the source. For these electrons the energy distribution  $N(E) \approx Q(E) \times t_0$  repeats the injection spectrum  $Q(E)$ . However, VHE  $\gamma$ -rays are produced by electrons of higher energies. In that case the spectrum of electrons is  $N(E) \approx Q(E) \times t_s$ . Then, besides of a less powerful injection rate  $Q \propto a^{-(1+\beta_2)/2}$  needed for explanation of the radio fluxes, the spectral intensity of these electrons is additionally suppressed by a factor  $a^2 \propto B_2^2$ . Therefore the intensity of VHE radiation depends on the magnetic field in zone 2 as  $f \propto B_2^{-(5+\beta_2)/2}$ , which is significantly stronger than at GeV energies. This is the result of emission of VHE electrons in the ‘saturation’ regime, when all the power injected in TeV electrons is channeled into (mostly) synchrotron and IC fluxes in the proportion defined by Eq.(12).

Thus, the flux of IC  $\gamma$ -rays could be significantly increased assuming *smaller* values of  $B_2$ , and hence also of  $B_1$  because the ratio of magnetic fields in two zones should be approximately at the level  $B_1/B_2 \sim 4$  in order to explain the radio data (see Paper 1). On the other hand,  $B_2$  cannot be significantly less than 0.3 mG, otherwise the bremsstrahlung flux would then exceed the radiation flux observed at  $E \sim 100$  keV, and the flux upper limit of EGRET at  $E \geq 100$  MeV (see Fig. 3). Note that this constraint on the magnetic field in the shell of Cas A imposed by the EGRET data are model independent since  $E \geq 100$  MeV  $\gamma$ -rays are produced by the same electrons with energies  $E_e \geq 1$  GeV which are responsible for the observed radio fluxes. On the other hand, the constraints imposed by the hard X-ray fluxes are to some extent conditional, being based on a (reasonable) assumption that the power-law injection spectrum starts from sub-MeV energies.

It is worthwhile to compare the constraints for the mean magnetic field in the shell, i.e.  $B_2 \geq 0.3$  mG, with the constraints imposed in the framework of a spatially homogeneous (i.e. a single-zone) model commonly used. Because radiative losses cannot steepen the spectrum of the radio electrons in Cas A, both the acceleration spectrum and the overall energy distribution of electrons  $N(E)$  at GeV energies should be steep, with a power-law index  $\beta_{\text{acc}} \geq 2.5$  for the mean power-law index of the observed radio fluxes  $\alpha \simeq 0.77$ . This is obviously much steeper than the index  $\beta_{\text{acc}} \simeq 2.2$  predicted by the two-zone model. As a result, the overall number of electrons predicted in the framework of such single-zone approach at low energies is much higher than for the two-zone model, and hence the lower limit for the mean magnetic field in the shell of Cas A consistent with the X-ray fluxes and upper flux limit increases to  $B_{\text{min}} \sim 1$  mG (e.g. Ellison et al. 1999). Both the steepness of the spectrum and the higher magnetic

field predicted in the framework of a single-zone model significantly reduce the fluxes of  $\gamma$ -rays to be expected at very high energies. Note that the impact of the steepness of the acceleration spectrum  $Q(E)$  can be significantly reduced in the framework of a more elaborated model where  $Q(E)$  becomes significantly flatter at higher electron energies, as in calculations by Ellison et al. (1999). However, there is no way to reduce the impact of the high mean magnetic field  $\geq 1$  mG which essentially reduces the number of multi-TeV electrons needed for production of a given flux of synchrotron X-rays. Therefore, in the framework of a single-zone model the fluxes of VHE radiation which would *not contradict* the observed hard X-ray flux will be significantly lower than the fluxes to be expected in the framework of a spatially inhomogeneous two-zone model (compare Fig. 5 with the results of Ellison et al. 1999, and Goret et al. 1999).

For the same values of the mean magnetic fields in zones 1 and 2, the fluxes of IC  $\gamma$ -rays expected from Cas A at TeV energies could be higher than in Fig. 5 if we consider a more structured model for the magnetic field distribution in the shell than the two-zone model. Namely, we may assume that the magnetic field in the shell of Cas A may decrease from the highest value  $B_1$  in the compact zone 1 (the acceleration sites) to a lower value  $B_2$  in the surrounding zone 2, and further on to some  $B_3 \leq B_2$  in zone 3. The chain of equations describing the energy distributions of particles in such 3-zone model is easily derived in the same way as described in Paper 1 for the 2-zone case. Note that the 3-zone modelling may be more adequate to the radio pattern of Cas A which shows significant variations in the brightness of the diffuse emission of the shell. Zone 3 would then represent the regions of the shell with relatively low magnetic field, as well as possibly the regions adjacent to the shell. Relativistic electrons could then escape from zone 2 into zone 3, as they do from zone 1 into zone 2. Because the spatial sizes of zone 2 are significantly larger than the sizes of the compact zone 1 structures, the characteristic timescales for the electron escape from zone 2 into zone 3 should be significantly larger than that the escape time from zone 1 into zone 2.

In Fig.6 we show the synchrotron radiation spectra calculated in the framework of the 3-zone model assuming that zones 2 and 3 have approximately the same volume filling factors in the shell. Note that zone 3 may include also regions not contained by the shell, in particular, the volume interior to the reverse shock if the diffusion coefficient there is sufficiently high (e.g. because of a low magnetic field there) so that relativistic particles would be able to significantly penetrate upstream of the freely expanding ejecta. In any case, zone 3 gives a principal possibility for high energy electrons to escape from zone 2 into a region with a lower magnetic field, resulting in some steepening of  $N_2(E)$  at  $E \geq 10$  GeV. Then it becomes possible to assume a power-law injection spectrum of the accelerated

particles (in zone 1) harder than  $\beta_{\text{acc}} \approx 2.2$ , without an excess of the radiation fluxes measured at  $6 \mu\text{m}$  (Tuffs et al., 1997).

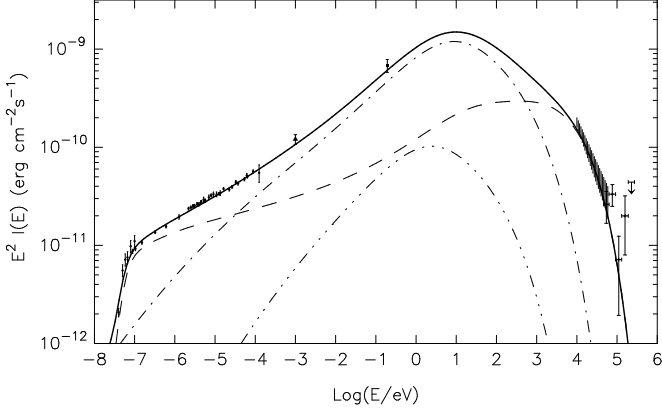


**Fig. 6.** The fluxes of synchrotron radiation calculated in the framework of the three-zone model, when the shell may contain regions with higher (zone 2) and lower (zone 3) magnetic fields. The fluxes produced in zones 1, 2 and 3, with the assumed magnetic fields  $B_1 = 1.6 \text{ mG}$ ,  $B_2 = 0.4 \text{ mG}$  and  $B_3 = 0.1 \text{ mG}$ , are plotted in dashed, dot-dashed, and 3-dot-dashed lines, respectively. The heavy solid line shows the total flux. The injection spectrum of the electrons in zone 1 is in the form of Eq.(4) with  $\beta_{\text{acc}} = 2.15$  and  $E_c = 17 \text{ TeV}$ ; the diffusive escape of electrons is described by  $\delta = 0.7$  for both zones 1 and 2, but  $\tau_{*,1} = 20 \text{ yr}$  for compact zone 1, and  $\tau_{*,2} = 800 \text{ yr}$  for the much larger zone 2.

In Fig. 7 we show the integral fluxes of IC  $\gamma$ -rays, in terms of  $E \times I(> E)$ , calculated in the framework of the 3-zone model, assuming 2 different values for the magnetic field in zone 1,  $B_1 = 1 \text{ mG}$  (solid line) and  $B_1 = 1.6 \text{ mG}$  (dashed line), the magnetic field  $B_2 = B_1/4$  in zone 2, and  $B_3 = 0.1 \text{ mG}$  in zone 3. Although  $B_1$  and  $B_2$  in these 2 cases change only by a factor 1.6, the fluxes of TeV  $\gamma$ -rays drop dramatically, by a factor of 6-7. Note that an assumption of the magnetic field  $B_3$  for zone 3 smaller than  $0.1 \text{ mG}$  does not result in a further increase of TeV  $\gamma$ -ray fluxes, because for such low magnetic fields all electrons up to several TeV are not in the “saturation” regime (see Eq.7), therefore variations of  $B_3$  do not affect the electron energy distribution  $N_3(E)$ .

It should be noted in connection with the 3-zone model, as compared with the 2-zone model, that it allows an increase of the  $\gamma$ -ray fluxes at energies above  $1 \text{ TeV}$  (where the IC radiation dominates the overall flux from electrons) by a factor of 3 assuming the same magnetic fields  $B_1$  and  $B_2$  for zones 1 and 2. Because the model parameters in zone 3 (as the magnetic field  $B_3$ , the volume  $V_3$  of zone 3 with this low field, and the escape time from zone 2 into zone 3) are difficult to deduce from radio observations, this introduces an additional uncertainty in the

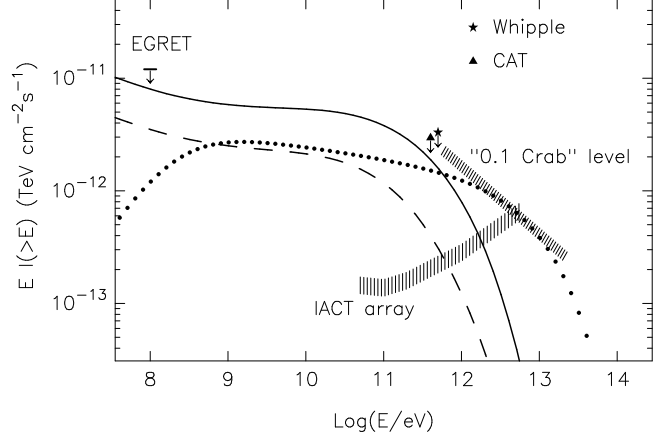


**Fig. 7.** The integral fluxes of the broad-band  $\gamma$ -radiation expected from Cas A in the case of two different values of the magnetic field in zone 1,  $B_1 = 1 \text{ mG}$  (solid line) and  $B_1 = 1.6 \text{ mG}$  (dashed line), calculated in the framework of a 3-zone model, assuming that  $B_2 = B_1/4$  in zone 2,  $B_3 = 0.1 \text{ mG}$ , and an injection of relativistic electrons with  $\beta_{\text{acc}} = 2.15$ . All other model parameters are the same as in Fig. 6, except for the exponential cutoff energy in the case of  $B_1 = 1 \text{ mG}$  for which  $E_c = 12 \text{ TeV}$  (in order to fit the X-ray fluxes for this magnetic field). The full dots show the fluxes of  $\pi^0$ -decay  $\gamma$ -rays calculated for relativistic protons with total energy  $W_p = 2 \times 10^{49} \text{ erg}$ , and acceleration spectrum with  $\beta_{\text{pr}} = 2.15$  and  $E_c = 200 \text{ TeV}$ , for a typical ‘H-atom’ gas density in the shell of Cas A about  $n_{\text{H}} = 15 \text{ cm}^{-3}$ . The level of fluxes corresponding to 10% of the flux detected from the Crab Nebula (e.g. Konopelko et al 1999), and the expected range of flux sensitivities of future IACT arrays for  $n_0 t = 10^3 \text{ h}$  (where  $n_0$  is the number of cells, see Aharonian et al. 1997) are also shown.

model predictions for the fluxes of VHE radiation. However, the mean magnetic fields  $B_2$  and  $B_1$  can be deduced rather accurately from future  $\gamma$ -ray detections of Cas A at lower energies (where bremsstrahlung dominates) as discussed in Sect. 2. Then in principle the spectral measurements of VHE  $\gamma$ -ray fluxes could give an important information about the parameters of zone 3 with low magnetic field.

The fluxes of TeV  $\gamma$ -rays on the level down to few per cent of the Crab nebula flux are in principle accessible for a system of Imaging Atmospheric Cherenkov Telescopes (IACTs) like the presently operating HEGRA. In this respect, the recent report of the HEGRA collaboration (Pühlhofer et al. 1999) about possible detection, at  $\sim 5\sigma$  significance level, of a weak signal from Cas A appears very interesting, and needs a further confirmation. It should be said that the extraction of a signal from Cas A would require special care, because the fluxes of IC  $\gamma$ -rays are expected to decline already at energies  $E \geq 0.5 \text{ TeV}$  much faster than the flux of the Crab Nebula, which is generally considered as a “standard candle”. This can be



seen in Fig. 7, as well as in Fig. 4 where the spectral index of the differential flux is plotted (to be compared with  $\alpha_{\text{dif}} \sim 1.5 - 1.6$  for the Crab Nebula). In Fig. 7 we also show the expected range of flux sensitivities of the forthcoming IACT arrays. It predicts that a significant flux of VHE  $\gamma$ -rays should be observed by the future VERITAS array (which is to operate in the northern hemisphere), if the observed fluxes of hard X-rays above 10 keV are indeed of synchrotron origin (Allen et al. 1997; Favata et al. 1997). Detection of the VHE  $\gamma$ -rays would allow a rather robust estimate of the mean magnetic fields  $B_1$  and  $B_2$ . This could be done by a modelling, rather than by a direct comparison of the X-ray and TeV  $\gamma$ -ray fluxes, because they are produced in different zones – in compact zone 1 and the diffuse ‘radio plateau’, respectively.

### 3.2. $\pi^0$ -decay gamma-rays

The TeV  $\gamma$ -radiation in Cas A could also be efficiently produced by relativistic protons and nuclei which should be accelerated simultaneously with the electrons. Our study of the spectral and morphological characteristics of the radio emission of Cas A does not favour the blast wave as an efficient accelerator of an electrons competitive with electron acceleration in the compact structures. However, there are no comparable observational constraints on the proton acceleration sites. In particular, the protons could plausibly be accelerated also at the blast wave. The standard theory of diffusive shock acceleration suggests that the hadronic component of cosmic rays could be accelerated much more copiously than the electrons, which generally explains the up to two orders of magnitude overabundance of the nucleonic component in the observed galactic cosmic rays.

In Fig.7 we show by full dots the  $\gamma$ -ray fluxes resulting from the decay of  $\pi^0$ -mesons produced by relativistic protons in the inelastic interactions with surrounding gas in the shell of Cas A. A power-law injection spectrum of relativistic protons in the form of Eq.(4), with  $\beta_{\text{acc}} = 2.15$  as for the electrons, is supposed. For the characteristic maximum energy of accelerated protons we have assumed  $E_c = 200$  TeV. Given the very high magnetic field in the acceleration region,  $B_1 \geq 1$  mG, even for a rather young age of Cas A the relativistic protons, not being affected by synchrotron losses like the electrons, can easily reach such high values of  $E_c$ . Indeed, using an estimate for the standard ‘parallel shock’ acceleration efficiency, the characteristic maximum energy of the protons accelerated during time  $t_0$  (e.g. see Lagage & Cesarsky, 1983) can be written as

$$E_c \simeq 450 \left( \frac{B}{1 \text{ mG}} \right) \left( \frac{t_0}{100 \text{ yr}} \right) \times \left( \frac{u_s}{3000 \text{ km/s}} \right)^2 \eta^{-1} \text{ TeV}, \quad (13)$$

where  $u_s \sim 3000$  km/s is a typical shock speed in Cas A (in particular, of the reverse shock), and  $\eta \geq 1$  is the so called gyrofactor (the ratio of the mean free path of a particle to its gyroradius). Thus, in the case of shock acceleration in the regime close to the Bohm diffusion limit,  $\eta \sim 1$ , the protons in Cas A could reach the energy of order 500 TeV during an acceleration time as short as  $t_0 \sim 100$  yr.

The total energy of relativistic protons assumed for the calculation of  $\pi^0$ -decay  $\gamma$ -ray fluxes in Fig. 7 is  $W_p = 2 \times 10^{49}$  erg, which corresponds to the mean injection power of the protons during  $t_0 \simeq 300$  yr of about  $L_p \simeq 2 \times 10^{39}$  erg/s. On the other hand, for the magnetic field  $B_1 = 1$  mG the acceleration power of the electrons is  $L_e = 5.5 \times 10^{38}$  erg/s, and  $L_e = 2.5 \times 10^{38}$  erg/s for  $B_1 = 1.6$  mG. Thus, the protons are supposed to be accelerated only by a factor of 4 – 8 more effectively than the electrons. This ratio cannot be increased further by more than a factor of 2, because otherwise the fluxes of TeV  $\pi^0$ -decay  $\gamma$ -rays would exceed the flux upper limits shown in Fig. 7. Therefore the ratio of proton to electron acceleration efficiencies in Cas A is significantly smaller than, or else have not yet reached, the high value  $\geq 40$  which is usually supposed for a typical source of the Galactic cosmic rays.

It is worth noticing that the upper limit to  $W_p$  imposed by the non-detection of TeV radiation from Cas A by Whipple and CAT detectors, is by one order of magnitude lower than the limitation imposed by the flux upper limit of the EGRET detector (see Fig. 7). Most probably, the total energy in accelerated protons in Cas A can be already now limited by a value not significantly exceeding  $10^{49}$  erg. Of course, we cannot exclude that relativistic protons are accelerated only to energies below the TeV range. This would then imply that the electrons as well are not accelerated to these energies, and therefore that the hard X-ray fluxes detected from Cas A are not of a synchrotron origin (which cannot be still ruled out, see Laming 1998). Thus, we expect that rather important conclusions could be derived already from the fact of, hopefully, further confirmation of the possible HEGRA detection of TeV  $\gamma$ -rays Cas A.

For both hadronic and electronic origin of the TeV  $\gamma$ -rays, the fluxes are to be produced in the extended shell of Cas A enclosed between angular radii 1.5 and 2.5 arcmin, or perhaps even in a bit larger region, if the VHE electrons would escape from the shell (this may compose a part of zone 3, as discussed in previous section). In terms of diameter, this makes an appreciable size of order of 5 arcmin. The IACT arrays are able to reconstruct the direction of individual  $\gamma$ -rays with an accuracy of several arcminutes which, in combination with a significant statistics of the  $\gamma$ -rays, may result in a principal possibility to localize relatively strong point sources with an accuracy of about 1 arcmin (Aharonian et al. 1997). Therefore IACT arrays operating at energies  $\sim 100$  GeV might be able in principle to see some structure (possible ‘hot spots’) in

the expected generally circular VHE  $\gamma$ -ray image of the source.

In this regard it might be worthwhile to note that radio observations of Kassim et al. (1995) at low frequencies show definite signs of the presence of a substantial mass (at least several  $M_{\odot}$ ) of cold gas in the central  $\leq 1'$  region of the Cas A. If TeV particles would be able to penetrate into that region (by diffusive propagation upstream of the freely expanding ejecta – in the case of high diffusion coefficient), then a central ‘hot spot’ would appear, associated with the bremsstrahlung and  $\pi^0$ -decay  $\gamma$ -rays produced by TeV electrons and protons illuminating the cold unshocked ejecta. The mean gas density of this ejecta in the central  $\leq 1'$  region of Cas A can be estimated as  $n_{\text{H}} \geq 10 \text{ cm}^{-3}$  per each solar mass of the ejecta (to be compared with the mean  $n_{\text{H}} \simeq 15 \text{ cm}^{-3}$  in the shell). Therefore, if the multi-TeV particles could really diffuse into that region, so that, say, 5 per cent of the total amount of these particles (protons and/or electrons) would be concentrated in that region, and the mass of freely expanding ejecta there could be about  $6 M_{\odot}$ , then one could expect that up to 20% of the total flux of VHE  $\gamma$ -rays would come from the centre of Cas A. Note that at energies  $\geq 100 \text{ GeV}$  where the sensitivity of IACT arrays is very high, most of the  $\gamma$ -ray flux produced by the electrons has a bremsstrahlung origin (see Fig.5).

Another possible ‘hot spot’ of the IC origin could appear (at higher energies) because of the known asymmetric spatial distribution of the target IR photons near the spectral peak around  $\sim 30 \mu\text{m}$  (see  $25 \mu\text{m}$  map by Dwek et al. 1987). If TeV electrons are distributed rather homogeneously in the shell, then the expected overall IC flux would not significantly change. However the image of Cas A at TeV energies will shift towards the position of maximum IR emission in the northern shell. If, on the other hand, the density of TeV electrons were enhanced in the northern shell (where the radio brightness is also enhanced) then we could expect an enhancement of the overall IC flux as well.

#### 4. Conclusions

Although not yet conclusively detected,  $\gamma$ -rays should inevitably be produced in Cas A by relativistic electrons which are responsible for the synchrotron radiation in the radio to submillimeter wavelengths. Our model calculations predict (Fig. 3) that the bremsstrahlung flux of these electrons should be observed at least at energies between 10 MeV and 30 GeV by the future GLAST detector. It is also possible that instruments like INTEGRAL or Astro-E will be able to detect the flux of bremsstrahlung photons at energies  $\geq 100 \text{ keV}$  (produced predominantly in the compact radio structures) from Cas A. In that case one expects to see a profound hardening of the radiation spectrum above 100 keV. But this effect could be detected only if the mean magnetic field  $B_1$  would not significantly ex-

ceed 1 mG, since otherwise the fluxes of soft  $\gamma$ -rays would fall below the limits of detectability of these instruments.

An important prediction of the spatially inhomogeneous model is that the spectra of accelerated electrons in Cas A correspond to a source function with a rather hard power-law index  $\beta_{\text{acc}} \sim 2.2$  (or even slightly harder), in agreement with predictions for efficient shock acceleration, and not a value of  $\beta_{\text{acc}} \sim 2.5$  as presently often assumed on the basis of the mean spectral index of the observed radio fluxes  $\alpha \approx 0.77$ . This prediction of the model can be directly tested by future detection of the  $\gamma$ -ray fluxes by GLAST in the energy region around 1 GeV. At these energies the total flux is dominated by the bremsstrahlung emission of electrons which escape from the compact acceleration regions into the surrounding shell, resulting in a power law distribution of electrons in the shell with an index  $\beta_2 = \beta_{\text{acc}}$ . Therefore, the spectral shape of the radiation detected at these energies will give direct information on the spectrum of acceleration in Cas A. The intensity of this radiation will give a rather robust estimate of the mean magnetic field  $B_2$  in the shell regions responsible for the diffuse ‘radio plateau’ emission. This would allow also a rather good estimate of the mean magnetic field in the compact radio structures,  $B_1 \sim 4 B_2$ .

Very important information on the magnetic field and chemical abundance of the gas in the compact radio structures can be derived by measuring the radiation fluxes at energies below 100 MeV. Although the expected angular resolution of GLAST may be insufficient to resolve the radio ring or radio knots, our study shows that most of the flux at these energies should be produced in these compact structures. Therefore, in combination with the known radio fluxes at low frequencies  $\nu \leq 40 \text{ GHz}$ , the  $\gamma$ -ray spectrum of Cas A at energies 10-100 MeV will provide an important information on the product of the gas parameters  $\overline{C_{\text{Z},1}}$  and  $n_{\text{H},1}$  in those structures. Adding also the information to be expected from the future high angular resolution measurements of the fluxes of thermal X-rays from the compact radio structures, even in the case of absence of line emission features it would be possible to disentangle  $n_{\text{H},1}$  and  $\overline{C_{\text{Z},1}}$ .

A synchrotron origin of the X-ray fluxes above 10 keV implies acceleration of the electrons beyond 10 TeV. If so, we could expect also noticeable fluxes of VHE  $\gamma$ -rays. These fluxes depend very sensitively on the mean magnetic field  $B_1$  in the compact regions of particle acceleration – the bright radio ring which is presumably connected with the reverse shock, and the radio knots –, and the field  $B_2$  in the diffuse radio plateau. The model prediction for these fields (based on interpretation of synchrotron fluxes only) corresponds to  $B_1 \sim (1 - 2) \text{ mG}$  and  $B_2 \sim B_1/4$ . For the case of low magnetic fields,  $B_1 \simeq 1 \text{ mG}$ , the integral flux  $I(> E)$  above 1 TeV makes about 5% of the Crab Nebula flux, and about (7 – 8)% above 300 GeV. The  $\gamma$ -ray spectrum produced by electrons due to bremsstrahlung and IC radiation is rather unusual: it is moderately hard

at  $E \leq 100$  GeV, with a photon index  $\alpha_{\text{dif}} \simeq 2.1 - 2.3$ , and quickly steepens to  $\alpha_\gamma > 3$  already at  $E \simeq 1$  TeV (see Fig.4). An increase of the magnetic field by only a factor of 2 results in a dramatic drop of the TeV  $\gamma$ -ray fluxes by one order of magnitude. Nevertheless, due to their high flux sensitivity and low detection energy threshold  $E_{\text{th}} \leq 100$  GeV (Aharonian et al. 1997), the IACT arrays should be able to detect the fluxes of VHE radiation of Cas A even in the case of high magnetic fields  $B_1 \simeq 2$  mG. The preliminary detection of Cas A by the less sensitive IACT system of HEGRA, reported by Pühlhofer et al (1999), strengthens this expectation.

In this regard, it is significant that in Cas A the expected  $\gamma$ -ray fluxes of hadronic origin should readily be distinguished from  $\gamma$ -rays of electronic origin due to the much steeper electronic spectra at energies above a few hundred GeV (see Fig.4). The spectral information on the VHE  $\gamma$ -ray flux can be obtained by the future VERITAS array, and might be also accessible to the HEGRA IACT system (depending on the magnetic fields  $B_1$  and  $B_2$ ) for  $\gamma$ -rays of the electronic origin, or if the total energy of relativistic protons in Cas A is not less than  $W_p^{(\text{max})} \simeq 2 \times 10^{49}$  erg. In both cases the predicted flux above 500 GeV is not much less than (0.05 – 0.1) ‘Crab’ (see Fig. 7). Note that the current upper flux limits reported by CAT (Goret et al. 1999) and Whipple (Lessard et al. 1999) telescopes put an upper limit to the total energy of relativistic protons in Cas A of  $W_p^{(\text{max})} \leq 5 \times 10^{49}$  erg (assuming acceleration of protons beyond TeV energies). A non-detection of  $\gamma$ -ray fluxes in the region above 100 GeV by future IACT arrays would imply that the efficiency of hadron acceleration in Cas A does not exceed the efficiency of electron acceleration.

*Acknowledgements.* The work of AMA has been supported through the Verbundforschung Astronomie/Astrophysik of the German BMBF under the grant No. 05-2HD66A(7).

## References

- Aharonian F. A., Hofmann W., Konopelko A. K., Völk H. J., 1997, *Astropart. Phys.* 6, 343; 369.
- Allen G.E., Keohane J.W., Gotthelf E.V., et al., 1997, *ApJ* 487, L97
- Anderson M., Rudnick L., Leppik P., Perley R., Braun R., 1991, *ApJ* 373, 146 (ARLPB)
- Anderson M.C., Rudnick L., 1996, *ApJ* 456, 234 (AR96)
- Atoyan A.M., Aharonian F.A., 1999, *MNRAS* 302, 253.
- Atoyan A. M., Tuffs R. J., Aharonian F. A., Völk H. J., 1999, *A&A*, in press; Paper 1.
- Bell A.R., Gull S.F., Kenderdine S., 1975, *Nature* 257, 463
- Bloom E.D., 1996, *Space Sci. Rev.* 75, 109
- Blumenthal G.R., Gould R.J., 1970, *Rev. Mod. Phys.* 42, 237.
- Braun R., Gull S.F., Perley R.A., 1987, *Nature* 327, 395.
- Chevalier R.A., Oegerle W.R., Scott J.S., 1978, *ApJ* 222, 527.
- Cowsik R., Sarkar S., 1980, *MNRAS* 191, 855.
- Dwek E., Petre R., Szymkowiak A., Rice W. L., 1987, *ApJ* 315, 571.
- Ellison D. C., Goret P., Baring M. G., Grenier I. A., Lagage P.-O., 1999, in *Proc. 26th ICRC (Salt Lake City)*, v. 3, p. 468.
- Esposito J.A., Hunter S.D., Kanbach G., Sreekumar P., 1996, *ApJ* 461, 820.
- Fabian A.C., Willingale R., Pye J.P., Murray S.S., Fabbiano G., 1980, *MNRAS*, 193, 175.
- Favata F., Vink J., Dal Fiume D., et al., 1997, *A&A* 324, L49.
- Fichtel C.E., Hartman R.C., Kniffen D.A., et al., 1975, *ApJ* 189, 163.
- Ginzburg V.L., *Theoretical Physics and Astrophysics*, Pergamon, Oxford, 1979.
- Goret P., Gouiffes C., Nuss E., Ellison D. C., 1999, in *Proc. 26th ICRC (Salt Lake City)*, v. 3, p. 496.
- Iyudin, A. F. et al., 1994, *A&A* 284, L1.
- Jansen F., Smith A., Bleeker J.A.M., de Korte P.A.J., Peacock A., White N.E., 1988, *ApJ* 331, 949.
- Kassim N.E., Perley R.A., Dwarakanath K.S., Erickson W.C., 1995, *ApJ* 455, L59.
- Konopelko A., Pühlhofer G., for HEGRA collaboration, 1999, in *Proc. 26th ICRC (Salt Lake City)*, v. 3, p. 444.
- Lagage P.O., Cesarsky C.J., 1983, *A & A* 118, 223.
- Laming J.M., 1998, *ApJ* 499, 309
- Lessard R. W., et al. 1999, in *Proc. 26th ICRC (Salt Lake City)*, v. 3, p. 488.
- Mezger P.G., Tuffs R.J., Chini R., Kreysa E., Gemuend H.-P., 1986, *A&A* 167, 145.
- Pühlhofer G., Völk H. J., Wiedner C. A. et al. 1999, in *Proc. 26th ICRC (Salt Lake City)*, v. 3, p. 492.
- Reed J.E., Hester J.J., Fabian A.C., Winkler P.F., 1995, *ApJ* 440, 706.
- The L.-S., Leising M.D., Kurfess J.D., Johnson W.N., Hartmann D.H., Gehrels N., Grove J.E., Purcell W.R., 1996, *A&AS* 120, 357.
- Tuffs R.J., 1986, *MNRAS* 219, 13.
- Tuffs R.J., Drury L. O’C., Fischera J., Heinrichsen I., Russel S., Völk H.J., 1997, *Proc. 1-st ISO Workshop on Analytical Spectroscopy (ESA SP-419)*, p.177.
- Vink J., Bloemen H., Kaastra J.S., Bleeker J.A.M., 1998, *A&A* 339, 201.
- Wright M., Dickel J., Koralesky B., Rudnick L., 1999, *ApJ* 518, 284.